Journal of Solid State Chemistry **154,** 130–136 (2000)
doi:10.1006/jssc.2000.8822, available online at http://www.idealibrary.com on IDEAL®

A Single-Crystal XRD and TEM Study of "$ScB_{17}C_{0.25}$"

A. Leithe-Jasper, L. Bourgeois, Y. Michiue, Y. Shi, and T. Tanaka[1]

National Institute for Research in Inorganic Materials, Namiki 1-1, Tsukuba, Ibaraki 305-0044, Japan

Received September 9, 1999; in revised form January 18, 2000; accepted January 30, 2000

In auxiliary metal fluxes (Si, Sn) at temperatures around 1650°C the crystal growth of "$ScB_{17}C_{0.25}$" was successfully performed. While in the Si flux agglomerates of whisker-like crystals are formed, the change to Sn significantly improved the quality of the columnar crystals with respect to size and surface smoothness. Based on single-crystal X-ray data collected on a four-circle diffractometer using Mo$K\alpha$ radiation and high-resolution transmission electron microscopy (HRTEM) the structure was solved by direct methods and refined to an reliability value R_1 of 0.055 for 661 $F_o > 4\sigma$ and 64 variables. The novel crystal structure belongs to the hexagonal system (space group *P6/mmm*), with lattice constants a, $b = 14.5501(15)$ Å and $c = 8.4543(16)$ Å and is formed by a framework based on B_{12} icosahedra which are radially connected to unusual "tubular" boron-based structural units. The Sc atoms reside on interstitial sites. In addition to the boron based clusters interstitial B atoms are found in the structure. The main structural features, which are governed by the arrangement of the boron clusters and the Sc atoms in the unit cell, could be unambiguously resolved by HRTEM, and simulated images match observed ones perfectly. © 2000 Academic Press

Key Words: **$ScB_{17}C_{0.25}$; crystal structure; scandium boro carbide; TEM; icosahedral boron clusters.**

1. INTRODUCTION

Recently a new scandium boro-carbide "$ScB_{17}C_{0.25}$" was found to exist (1). This phase was also identified in the systematic investigation of an isothermal section of the Sc–B–C system at 1700°C (2). From electron diffraction and full indexing of powder XRD patterns a hexagonal unit cell a, $b = 14.4763(14)$ Å and $c = 8.9375(4)$ Å was deduced. No systematic extinctions were observed. $ScB_{17}C_{0.25}$ was found to exhibit a considerable field of homogeneity: $ScB_{16.5+x}C_{0.2+y}$ with ($x \leq 2.2$ and $y \leq 0.44$). Since the powder pattern of this phase showed a very strong low-angle diffraction peak ($d_{100} = 12.54$ Å) and the compound is basically composed of the light elements B, Sc, and C a further investigation of the crystallization properties was carried out. This was motivated by the recent successful installation of YB_{66} in form of single-crystal monochromators in soft X-ray synchrotron beam lines (3,4). To develop the second generation of state-of-the-art X-ray monochromators that should show improved properties in terms of thermal and electrical conductivity, considerable effort is currently being undertaken to modify the properties of YB_{66} as well as to find suitable other new materials with better performance, especially for use in high-flux beam lines. In terms of new YB_{66}-related materials recently the ternary boride $YB_{41}Si_{1.2}$ (5,6) was grown in form of large single crystals. This clearly demonstrated that by addition of small amounts of a third element to the rare earth borides new ternary structures can be formed. To replace Y with a lighter element while keeping the refractory icosahedral boron-based framework of structure is therefore the ultimate task for modifying the properties of the monochromator materials in terms of thermal conductivity and background fluorescence emission. Thus the search for new materials now mainly concentrates on Sc-based materials. Sc, representing a rather light element ($Z = 21$) with properties close to transition metals, as well as rare earth metals, can form boron-rich compounds if small additions of carbon are allowed (2). It was also found that the phase melts incongruently, which backed the assumption that this material could be grown in form of large crystals from a molten zone of appropriate composition (1,2). However the fabrication of large crystals by means of floating zone melting or Czochralski pulling from the melt turned out to be by no means straightforward since the compound showed a very pronounced tendency to crystallize in the form of bundles of whiskers from the melt. This made a stable crystal growth impossible. Therefore we attempted to grow crystals of this compound by the solution growth method. This is a rather versatile method since solute/solvent ratio, temperature profiles, and solvent materials can be varied.

[1] To whom correspondence should be addressed. E-mail: tanakat@nirim.go.jp.

0022-4596/00 $35.00

2. EXPERIMENTAL PROCEDURES

2.1. Crystal Growth

The powder XRD patterns of arc-melted samples containing $ScB_{17}C_{0.25}$ and Si were encouraging, showing no obvious change in the lattice of the compound. This was interpreted as that Si does not suppress the formation of this phase and therefore can be used as a flux. A likely solubility of Si in the boro-carbide structure was accepted since no obvious influence on the symmetry of the lattice was observed in these experiments.

Starting materials for the crystal production were powders of ScB_{17} and $ScB_{17}C_{0.25}$ that were synthesised by boro thermal reduction (in a BN crucible inserted in an inductively heated carbon-free TiB_2/BN composite susceptor under dynamic vacuum) according to the reaction

$$Sc_2O_3 + (2m + 3)B \rightarrow 2ScB_m + 3\,BO\uparrow$$

at temperatures up to 1700°C. (Sc_2O_3 powder, 3N, Crystal Systems Inc., Japan; amorphous boron, 3N, SB-Boron Inc., USA; and graphite powder, 3N, Koujundo Kagaku Co., Japan).

Then the desired amount of carbon was added to the powdered sample and fired again at 1700°C in a graphite susceptor. Crystal production in a Si flux (Si, 99.96 wt.%, 325 mesh, Cerac Inc., USA) was carried out under a flow of Ar gas by inductively heating a mixture of weight ratio 1 : 4 of $ScB_{17}C_{0.25}$ and Si in a BN crucible in a graphite susceptor to 1700°C (the temperature was measured using an optical pyrometer (0.65 μm) by simulating blackbody conditions through a small drilled hole in the crucible lid), keeping it there for several hours, and slowly cooling it (25°C/h) to 1300°C. The Si flux was dissolved by keeping the material in a $HNO_3/HF/H_2O$ (1 : 1 : 3) mixture at 80C for 36 h. These experimental conditions were sufficient to dissolve most of the Si but inflicted no visible damage on the crystals. Agglomerates of whisker-like crystals were found. Thus the flux growth from Si resulted in no favorable change in the crystal morphology. To overcome these undesired agglomerations of very thin crystals, Si was replaced by Sn.

The crystal growth in a tin flux was performed by mixing ScB_{17} with tin powder (Sn, 3N, 100mesh, Rare Metallic Co. Ltd., Japan) in a weight ratio of 1:10 and inductively heating the compacted sample in a BN crucible inside a graphite susceptor under a flow of Ar gas to 1600°C for 8 h. After the power was switched off the system was allowed to cool down to room temperature under Ar gas flow (usually within 2 h). The tin matrix was dissolved by warm

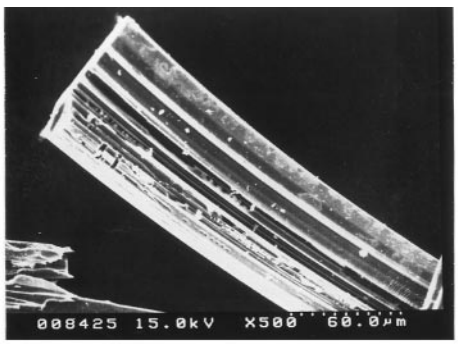

(a)

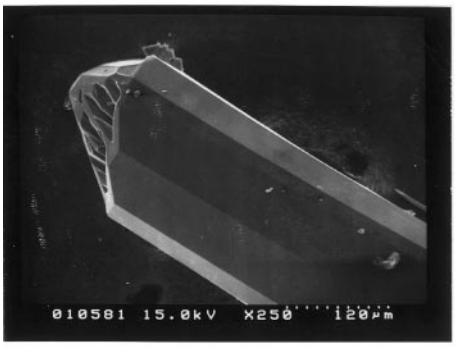

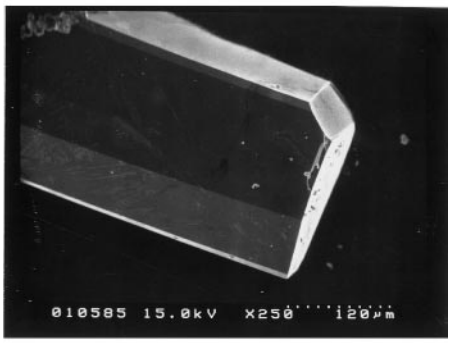

(b)

FIG. 1. Morphologies observed for $ScB_{17}C_{0.25}$ crystals. (a) Si flux and (b) Sn flux.

concentrated HCl leaching. Silver-gray well-developed columnar crystals with a metallic lustre with a size up to $1 \times 0.1 \times 0.1$ mm were isolated. The interesting fact in these experiments is that carbon was obviously supplied in the form of CO/CO_2 (small amounts of oxygen within the experimental setup reacted with the hot graphite susceptor) via the gas phase followed by reduction and solution in the liquid tin. As pointed out in previous publications (1,2) only a very small amount of carbon is sufficient and necessary to stabilize the $ScB_{17}C_{0.25}$ phase, which easily forms under "noncarbon-free" experimental conditions during synthesis of higher borides of Sc. Figure 1 shows SEM pictures of some representatives of the obtained crystals.

2.2. Characterizations

The chemical composition of several crystals grown in the Sn flux were checked by EPMA. Standards in the form of a ScB_{12} crystal and a $B_{4.5}C$ crystal (the compositions were established by wet chemical analysis) were used to deduce the composition. Special attention was paid to possible Sn inclusions. The compositions of the crystals were found to lie in the range of $ScB_{16}C_{0.69}$ and $ScB_{17.4}C_{0.6}$ which was accepted in accordance to prior results for $ScB_{17}C_{0.25}$ based on wet chemical analysis (1). No Sn could be detected in the crystals.

Several columnar (Sn flux) and thin needle-shaped (Si flux) specimen were mounted on a Weissenberg camera (Ni-filtered Cu$K\alpha$ radiation). The crystals were aligned parallel to the long axis. Rotation photographs revealed that the preferred growth direction of the material lies along the short c axis of the hexagonal unit cell. Equiinclination Weissenberg photographs of several layers were recorded showing a reciprocal space of hexagonal symmetry without any special extinctions. Thus the results of the initial electron diffraction and powder XRD analysis (1) proved to be correct.

Since crystals grown by Sn flux were larger and of higher quality than the specimens grown in Si flux the final data collection was performed on one of them on a Rigaku AFC7R rotating anode four-circle diffractometer (data collection at 60 kV and 200 mA, Mo$K\alpha$). This data set was used for the refinement of the structure presented here. Intensity data were corrected for Lorentz and polarization effects. Details of the XRD analysis are given in Table 1.

The high-resolution transmission electron microscopy (HRTEM) and electron diffraction observations were carried out on a field-emission JEM-3000F (JEOL) instrument operated at 300 kV. HRTEM image simulations by the multislice calculation method were performed using the MacTempas simulation package with the appropriate electron optical parameters of our microscope. The simulated images presented herein were chosen near the Scherzer defocus of -590 nm, and for the crystal thickness resulting in the best match with the experimental image.

TABLE 1
Crystallographic and Collection Data of $ScB_{17}C_{0.25}$

Crystal system	Hexagonal
Space group	$P6/mmm$ (No. 199)
a (Å)	14.5501(15)[a]
c (Å)	8.9543(16)[a]
c/a	0.6154
Volume (Å^3)	1641(1)
Z	12
fw	232.1
D_x (g/cm^3)	2.817
Applied radiation, λ (Å)	Monochrom. Mo$K\alpha$, 0.71073 Å
Scan mode	$\omega/2\theta$
Linear absorption coefficient μ (mm^{-1})	1.25
Crystal dimensions (mm)	$0.25 \times 0.075 \times 0.075$
Absorption correction	Empirical (ψ scans)
Data corrections	Lorentz, polarization
Reflections range	$0 \le h \le 17$ $0 \le k \le 10$ $0 \le l \le 12$
$2\theta_{max}$ (°)	59.77
Total number of reflections	878
Unique reflections	878
Structure solution, refinement Programs	SIR92, SHELX97 (based on F_o^2)
Number of variables	64
R_1^b [$F_o > 4\sigma(F_o)$] (for 661 F_o)	0.055
R_1 [all F_o] (for 878 F_o)	0.081
wR_2 (F^2)[b]	0.165

[a] The lattice constants were obtained on the four-circle diffractometer.
[b] $R_1 = \sum||F_o| - |F_c||/\sum|F_o|$; $wR_2 = [\sum|w(F_o^2 - F_c^2)^2|/\sum|w(F_o^2)^2|]^{1/2}$, $w = [\sigma^2(F_o^2) + (xP)^2 + yP]^{-1}$, where $P = (\mathrm{Max}(F_o^2, 0) + 2F_c^2)/3$.

3. RESULTS AND DISCUSSION

3.1. Determination of the Structure

The very small amount of C necessary to form this boron-rich compound already suggests the possibility of an icosahedral B_{12} boron-cluster-based structure in accordance with many reported crystal structures of higher binary and ternary borides incorporating transition metals, rare earth metals, and light atoms such as B, C, and Si in interstitial sites of complex three-dimensional boron-based frameworks (7–11).

With the previously mentioned significant homogeneity range and flotation densities of 2.65(5) g/cm^3 (measured on crystals grown by the Sn flux), $Z = 12$ formula units were assumed. The structure was solved by applying direct methods of the SIR92 program (12) to the data set assuming only Sc and B atoms in the unit cell, thus neglecting C at this

stage of investigation. The refinement was carried out with the SHELX97 (13) program package. After the positions of the "heavy" Sc atoms were assigned, the boron framework structure was found in a stepwise process within hexagonal symmetry of space group *P*6/*mmm* (no. 191). The positions of the Sc atoms in the 12o (x, $2x$, z) site with $z \approx 0.75$ and the rather short c axis already indicated that the boron framework could only be accommodated between these metal layers. As already mentioned, no extinction rules were observed in the electron and single-crystal diffraction data; thus a rhombohedral lattice of B icosahedra could be ruled out. The first boron-based arrangement ascending from the accumulation of possible positions was a very unusual one, where boron atoms seemed to form six-membered interconnected rings (denoted in this paper as type III polyhedron), establishing tube-like arrangements along the unit cell's c axis. The refined III polyhedron, thus forming B_{12} hexagonal antiprisms, is centered along the c axis at (2*e*) (Wyckoff position) (0, 0, $\sim$0.25). This arrangement gives rise to the formation of tubular (diameter of 3.8 Å) channels that are the key feature of this crystal structure. Nevertheless in "BeB_3" (the only higher boride compound exhibiting hexagonal symmetry prior to the discovery of $ScB_{17}C_{0.25}$) (14,15) a similar arrangement of boron atoms is observed to exist. Rings of boron atoms form tube-like structures in which some extra atoms were found to reside. By geometrical considerations under constraint of assumed icosahedral cluster formation two types of boron icosahedra (I, II) were found to exist in the $ScB_{17}C_{0.25}$ structure. The I, II icosahedra are centered at (6*l*) (0.2042, $-$0.2042, 0) and (6*k*) (0.3429, $-$0.3429, $\frac{1}{2}$), respectively. Distortions of these icosahedra are small: in the I icosahedron, intraicosahedral boron bond lengths are in the range $1.764 \leq d_{BB} \leq 1.881$ Å with an average $d_{BB} = 1.818$ Å for the triangular faces of the icosahedron. With an average angle of 59.93° for the triangular faces of I, deviance from the ideal value of 60° in a regular icosahedron is small. Similar is the situation for icosahedron II: intraicosahedral boron distances are in the range of $1.741 \leq d_{BB} \leq 1.833$ Å with an average value of $d_{BB} = 1.798$ Å and an average triangular angle of 60.15°. During the refinement of the crystal structure no indication of a boron–carbon substitution and deviation from full occupancy of the icosahedral boron atoms were observed. They form large six-membered rings of mutually inclined and interconnected icosahedra that are bonded to the tubular central cores around the c axis. This arrangement easily combines the tubular character with the layer-like arrangement of the metal atoms. The rest of the boron atoms were found to reside in interstices formed by the Sc atoms as well in the form of atoms bridging the rings of boron icosahedra. The structure is outlined in Figs. 2–4. The atomic positions are given in Table 2. Interatomic distances are all in the

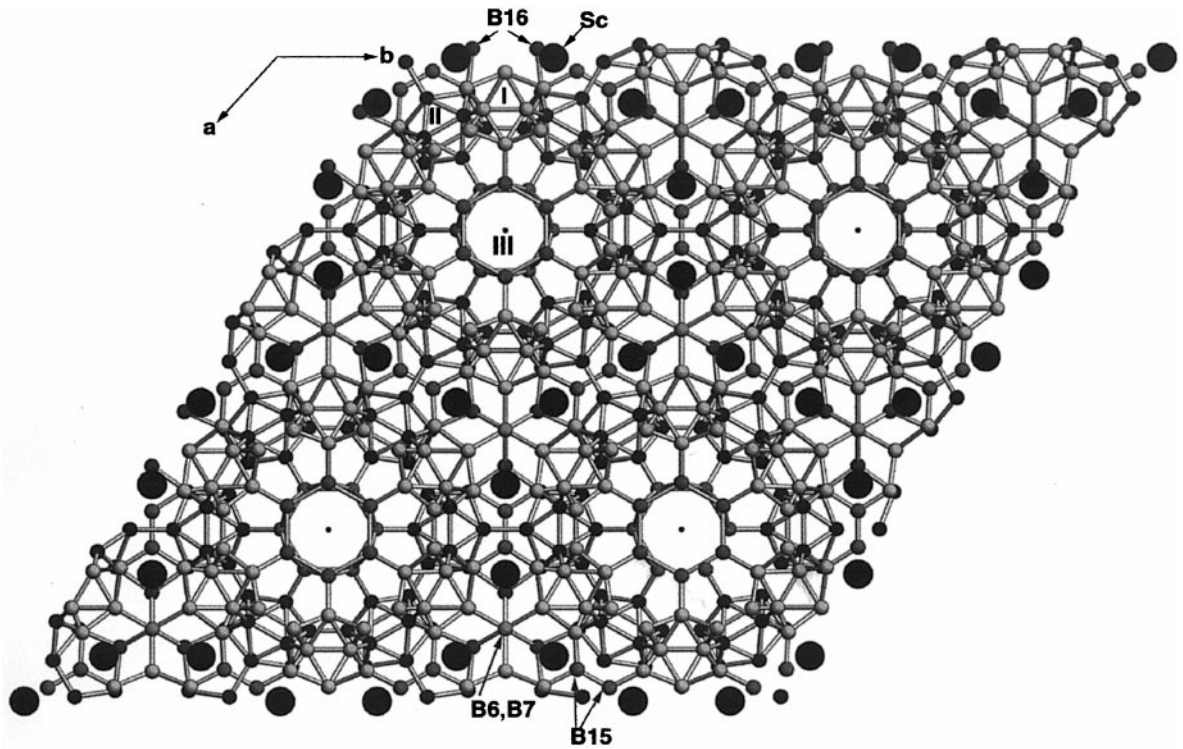

FIG. 2. The polyhedral network in $ScB_{17}C_{0.25}$ viewed along the c axis. Boron-based B_{12} icosahedra I and II arranged around B_{12} hexagonal antiprisms III and Sc atoms are outlined.

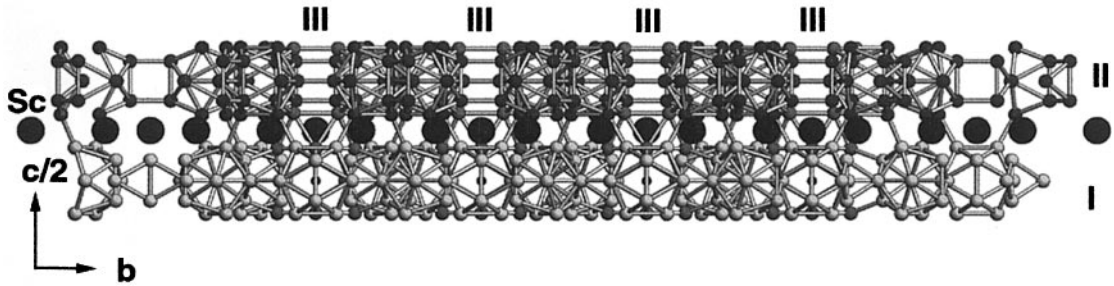

FIG. 3. The polyhedral network in $ScB_{17}C_{0.25}$ viewed normal to the *b* axis. The layers of B_{12} I and II icosahedra, Sc atoms, and interstitial atoms are depicted.

usual range of lengths observed in higher borides (1.6 to 1.95 Å) and are listed in Tables 3a–3d. Intraicosahedral bond lengths are slightly longer than intericosahedral bondlengths, also in agreement with other structures based on this kind of boron clustering. Similar to the case of $YB_{41}Si_{1.2}$ (5) an unusual inter B_{12}(II) connection in form of a square of B atoms is observed (see Fig. 5), violating the usual bond formation tendency along the fivefold axes of the icosahedra. From the present state of analysis no specific position exclusively occupied by C could be assigned. Bond length considerations, abnormally low-temperature factors, and a higher charge density led us to refine the B15 and B16 positions in the form of a mixed occupancy by B and C.

It therefore seems that the very small amount of carbon (less than 2 wt.%!) that is necessary to stabilize this crystal structure is more or less diluted over a few interstitial sites. This remains a puzzling aspect of this rather unusual new crystal structure. The most striking feature of this boron framework is the "tubes" along the unit cell's *c* axis formed by interconnected rings of boron atoms. They form long channels within the structure. Since the morphologies of the crystals seem to be rather independent of the growth methods applied, a correlation of the crystal structure and crystal shape could be assumed. The experimental findings suggest that growth along the "tubular" *c* axis seems to be energetically much more favorable than a lateral increase of the crystals via growth in the *a*–*b* plane of the structure. Analysis of the difference Fourier maps indicate the possibility of atoms distributed within these channels. They are denoted B17 and B18 in Table 2 with rather large thermal factors and only partial positional occupation (53% for B17 and 67% for B18), reflecting rather high local disorder.

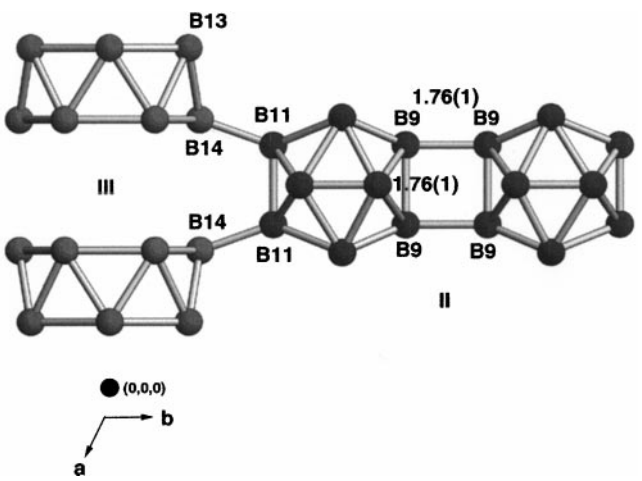

FIG. 4. Connection of the "tubular" III polyhedron with the II B_{12} icosahedron depicting the unusual type of linkage. An approximately square plane is formed by the connection of four apical B atoms.

TABLE 2
Atomic Coordinates and Isotropic Displacement Parameters of $ScB_{17}C_{0.25}$

Atom	Site	Polyh.	*x*/*a*	*y*/*a*	*z*/*c*	U (Å$^2 \times 10^3$)
Sc1[a]	12o		0.4251(1)	0.8502(1)	0.7496(2)	5.8(4)
B1	12p	I	0.6699(4)	0.7362(4)	0.0	3.2(9)
B2	12p	I	0.5300(4)	0.6629(4)	0.0	6.4(9)
B3	24r	I	0.5985(3)	0.7380(3)	0.8351(4)	3.7(7)
B4	12o	I	0.1419(7)	0.2838(5)	0.9011(6)	6.6(9)
B5	12o	I	0.5242(4)	0.2621(2)	0.0986(4)	4.3(9)
B6	4h		$\frac{1}{3}$	$\frac{2}{3}$	0.8288(10)	5 (2)
B7	4h		$\frac{1}{3}$	$\frac{2}{3}$	0.6165(10)	5 (2)
B8	24r	II	0.3077(3)	0.9274(3)	0.6661(4)	4.4(7)
B9	12g	II	0.4395(4)	0.0	0.5984(6)	5.3(8)
B10	12q	II	0.5375(5)	0.6562(5)	$\frac{1}{2}$	6 (1)
B11	12n	II	0.7571(4)	0.0	0.5995(6)	5.0(9)
B12	12q	II	0.2266(5)	0.3405(4)	$\frac{1}{2}$	6 (1)
B13	12o	III	0.0771(2)	0.1542(5)	0.8347(7)	4 (1)
B14	12n	III	0.1327(4)	0.0	0.6664(7)	8 (1)
B15[b]	6l		0.4694(3)	0.9388(7)	0.0	8 (1)
B16[c]	6m		0.3944(6)	0.7888(7)	$\frac{1}{2}$	13 (1)
B17	6l		0.0391(12)	0.0782(24)	0.0	45 (8)
B18	6m		0.0379(10)	0.0758(10)	$\frac{1}{2}$	44 (6)

[a] Isotropic U_{eq} (one-third of the trace of the orthogonalized U_{ij} tensor); thermal factor $T = \exp(-8\pi^2 U[\sin(\theta)/\lambda]^2)$.
[b] Mixed occupancy: 27%C, 73%B.
[c] Mixed occupancy: 20%C, 80%B.

TABLE 3

Central atom	Ligands	Distances (Å)	Central atom	Ligands	Distances (Å)
(a) Bonds between atoms within the B_{12}(I) Icosahedron. Center of icosahedron: (6*l*) (0.2042, −0.2041, 0.0)					
B1	B2	1.764(5)	B4	B4	1.77(1)
	2 B4	1.786(6)		2 B1	1.786(6)
	2 B3	1.814(5)		2 B3	1.827(7)
B2	B1	1.764(5)	B5	B5	1.77(1)
	2 B3	1.812(5)		2 B2	1.859(6)
	2 B5	1.859(6)		2 B3	1.881(6)
B3	B3	1.781(8)			
	B2	1.812(5)			
	B1	1.814(5)			
	B4	1.827(7)			
	B5	1.880(6)			
(b) Bonds between Atoms within the B_{12}(II) icosahedron. Center of icosahedron: (6*k*) (0.3429, −0.3429, $\frac{1}{2}$)					
B8	2 B8	1.770(6)	B11	B11	1.78(1)
	B12	1.805(5)		2 B12	1.790(6)
	B9	1.813(5)		2 B8	1.833(6)
	B11	1.833(6)			
B9	B9	1.76(1)	B12	B10	1.741(9)
	2 B8	1.769(6)		2 B11	1.790(6)
	2 B10	1.814(6)		2 B8	1.805(5)
B10	B12	1.741(9)			
	2 B8	1.813(5)			
	2 B9	1.814(6)			
(c) Bonds between atoms within the B_{12}(III) antiprism. Center of polyhedron: (2*e*) (0.0, 0.0, 0.2494) and next nearest neighbors for Sc					
B13	2 B13	1.943(6)	B14	2 B13	1.809(5)
	2 B14	1.809(5)		2 B14	1.930(6)
Sc	1 B16	2.3738(34)			
	1 B6	2.4197(30)			
	2 B9	2.4844(39)			
	2 B5	2.5036(34)			
	1 B15	2.5049(39)			
	2 B3	2.5684(39)			
	2 B8	2.5792(40)			
	1 B7	2.6025(56)			
	2 B2	2.6536(34)			
	2B10	2.6715(35)			

(d) Bonds between polyhedra and to isolated atoms

Polyhedra	Bond	Distances (Å)	Polyhedra	Bond	Distances (Å)
I–I	B1–B1	1.67(1)	III–*x*	B13–B17	1.77(2)
I–II	B3–B8	1.741(5)	III–*x*	B14–B18	1.92(1)
I–III	B4–B13	1.739(8)			
I–*x*[a]	B2–B15	1.669(8)			
I–*x*	B5–B6	1.909(6)			
II–II	B12–B12	1.64(1)			
II–II	B9–B9	1.76(1)			
II–III	B11–B14	1.713(8)			
II–*x*	B10–B16	1.846(9)			

[a] *x* denotes isolated atom.

3.2. *HRTEM Results for "ScB $_{17}C_{0.25}$"*

Figures 5a and 5b show HRTEM images and electron diffraction patterns taken along the [0001] and [11$\bar{2}$0] directions, respectively. In (a), which shows a projection along the [0001] axis of the (*a*, *b*) plane of the crystal, the main structural features obtained from X-ray diffraction are imaged. The 12-membered rings of white dots, 12.5 ± 0.1 Å in diameter, correspond to the Sc atom rings. The white dot surrounded by a dark ring approximately 3.2 Å in diameter can be interpreted as the channel defined by boron hexagonal antiprisms aligned with their sixfold axis along the [0001] direction of the crystal. The larger black ring, sand-

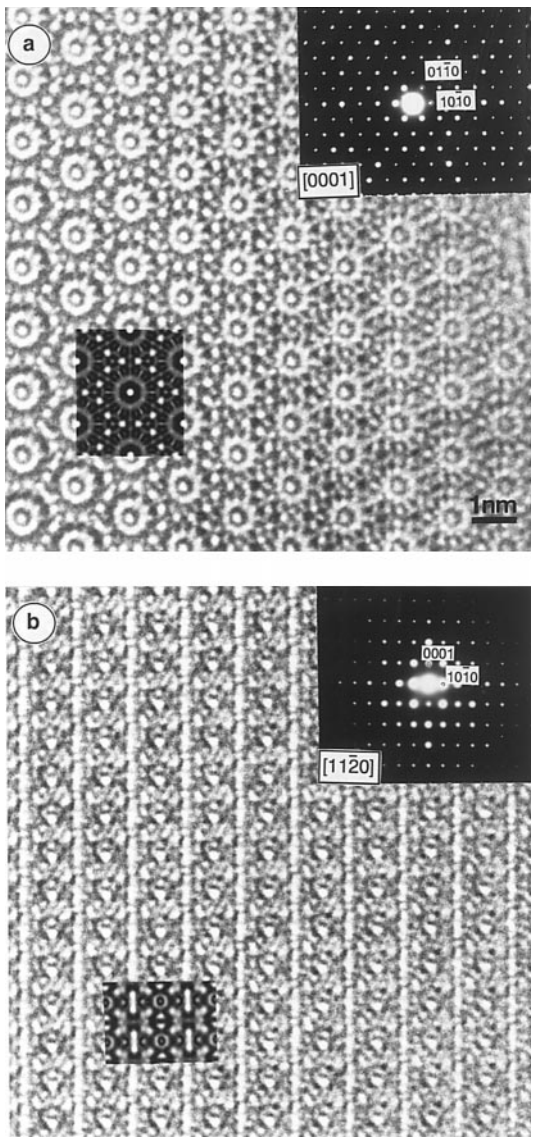

FIG. 5. (a) HRTEM images and electron diffraction patterns taken along the [0001] direction. (b) HRTEM images and electron diffraction patterns taken along the [11$\bar{2}$0] direction.

wiched between the Sc ring and the 3.2-Å ring, reflects the presence of the 12 boron icosahedra (I, II) bonded to the central tubular region. Comparison with the simulated image (see inset) allows one to confirm the above interpretation. Agreement between the computed and the experimental images is good, particularly considering the complexity of the structure model. The fact that the value measured on the HRTEM picture for the channel diameter is smaller than 3.8 Å may be attributed to the incident electron beam not being perfectly parallel to the [0001] axis; this may be compounded by a slight departure from optimum defocus of the objective lens. The different image details on the right-hand side of Fig. 5a, which is very close to the edge of the specimen, arise from a decrease in thickness; this effect could be reproduced in the simulations. The presence of channels along [0001] is also apparent in Fig. 5b, where they are imaged as almost continuous white lines with a constant separation of 12.5 ± 0.1 Å The black dots surrounded by a white ring visible in both calculated and experimental images may be ascribed to higher densities of Sc atoms along the $[11\bar{2}0]$ direction.

ACKNOWLEDGMENTS

A. L.-J., L.B., and Y.S. acknowledge support via a STA fellowship. The fast and reliable work of the NIRIM technical support group is highly appreciated.

REFERENCES

1. T. Tanaka, *J. Alloys Compds.* **270,** 132–135 (1998).
2. Y. Shi, A. Leithe-Jasper, and T. Tanaka, *J. Solid State Chem.* **148,** 250–259 (1999).
3. Y. Kamimura, T. Tanaka, S. Otani, Y. Ishizawa, Z. U. Rek, and J. Wong, *J. Crystal Growth* **128,** 429 (1993).
4. J. Wong, G. N. George, I. J. Pickering, Z. U. Rek, M. Rowen, T. Tanaka, G. H. Via, B. DeVries, D. E. W. Vaughan, and G. E. Brown Jr., *Solid State Commun.* **92,** 559 (1994).
5. I. Higashi, T. Tanaka, K. Kobayashi, Y. Ishizawa, and M. Takami, *J. Solid State Chem.* **133,** 11–15 (1997).
6. T. Tanaka, S. Okada, and Y. Ishizawa, *J. Solid State Chem.* **133,** 55–58 (1997).
7. V. I. Matkovich, G. V. Samsonov, P. Hagenmueller, and T. Lundstroem, (Eds.), "Boron and Refractory Borides," Springer-Verlag, Berlin, 1977.
8. G. A. Slack, C. I. Hejna, M. Garbauskas, and J. S. Kasper, *J. Solid State Chem.* **76,** 52–86 (1988).
9. R. Naslain, A. Guette, and P. Hagenmueller, *J. Less Common Met.* **47,** 1–16 (1976).
10. P. Rogl, *in* "Phase Diagrams of the Ternary Metal-Boron-Carbon Systems" (G. Effenberg, Ed.). ASM International, 1998.
11. M. Vlasse, G. A. Slack, M. Garbauskas, J. S. Kasper, and J. C. Viala, *J. Solid State Chem.* **63,** 31–45 (1986).
12. A. Altomare, G. Cascarano, C. Giacovazzo, A. Guagliardi, M. C. Burla, G. Polidori, and M. Camalli, *J. Appl. Cryst.* **27,** 435 (1994).
13. G. M. Sheldrick, "SHELX97: A Programme for the Solution and Refinement of Crystal Structures," Universitaet Goettingen, Goettingen, Germany, 1997.
14. R. Mattes, K. F. Tebbe, H. Neidhard, and H. Rethfeld, *J. Less Common Met.* **47,** 29–32 (1976).
15. R. Mattes, K. F. Tebbe, H. Neidhard, and H. Rethfeld, *Z. Anorg. Allg. Chem.* **413,** 1–9 (1975).